

Water hydraulics, retention and repellency, response to soil texture, biochar pyrolysis conditions and wetting/drying

Oluwaseun Temitope Faloye^{1,2,3*}, Ebenezer Ayodele Ajayi^{4,5,3}, Jens Rostek³, Toju Babalola², Abayomi Fashina⁶, and Rainer Horn³ 

¹Department of Agricultural and Biosystems Engineering, LandMark University, PMB 1001, Omu Aran, Kwara State, Nigeria

²Department of Water Resources Management and Agrometeorology, Federal University, PMB 373, Oye-Ekiti, Ekiti State, Nigeria

³Institute for Plant Nutrition and Soil Science, Christian Albrechts University zu Kiel, Hermann Rodewaldstr. 2, 24118 Kiel, Germany

⁴Department of Agricultural and Environmental Engineering, Federal University of Technology, PMB 704, Akure, Nigeria

⁵Department of Food and Biosystems Engineering, Afe Babalola University, PMB 5454, Ado Ekiti, Nigeria

⁶Department of Soil Science and Land Resources Management, Federal University, PMB 373, Oye Ekiti, Nigeria

Received March 9, 2022; accepted June 14, 2022

Abstract. Studies which evaluated the aggregation effects in biochar-amended soils by determining the saturated hydraulic conductivity and water repellency, in combination with wetting/drying scenarios are rare. Therefore, the objective of this study is to link water repellency and water retention in biochar-amended soils to the aggregation effect under different pyrolysis conditions and soil textures. Two feedstock sizes; twig and branch-based mango were pyrolysed at 550°, and were then mixed with sandy loam and silt loam at application rates of; 0, 30, 45 and 60 g kg⁻¹ respectively. Sequentially, the soil-biochar mixtures were subjected to five wetting and drying cycles. In each of the cycles, the saturated hydraulic conductivity, and thereafter the contact angles of the soil-biochar mixtures were measured using the sessile drop approach. The results showed that biochar addition decreased the saturated hydraulic conductivity in all cycles. The rigidity effect was more pronounced in soil amended with biochar and produced using twig mango as opposed to the biochar produced using mango branch. A higher rigidity value was measured in the silt loam and sandy loam amended with twig as compared to the branch-based mango which may be attributed to aggregation processes. This also coincides with higher contact angle values and water retention values that were measured using twig as opposed to branch-based mango.

Keywords: soil amendment, contact angle, aggregation, saturated hydraulic conductivity, pore-size distribution, pyrolysis conditions

INTRODUCTION

Biochar is a carbonaceous substrate derived from the pyrolysis of organic material. It has steadily gained in popularity as a subject of scientific study because of its potential for the long-term sequestration of carbon in soils and its beneficial effect as a soil amendment. Whereas there is a wide consensus concerning the potential of biochar as a means to sequester carbon into soil (Woolf *et al.*, 2010), its secondary effects on soil properties (hydrophysical and structural) are often still widely debated. This may be related to several factors that determine biochar properties and thus, its impact on amended soil. Factors such as the feed stock type and size, pyrolysis condition (temperature and residence time) are known to determine biochar attributes / quality, while the soil properties (dominant minerals and texture), land use management, biochar particle size and climate determine, among other factors, the biochar reaction in the soil (de Jesus Duarte *et al.*, 2019; Demirbas, 2004; Guo and Lua, 1998; Lua *et al.*, 2004).

In general, when biochar is added to the soil, some physical properties, including surface area, porosity, pore-size distribution (PSD) and texture are modified, which ultimately alters the soil's water storage capacity and availability (Baiaomonte *et al.*, 2019). However, the reaction depends on the attributes of the biochar, like feedstock type,

size and pyrolysis condition (temperature) (Kameyama *et al.*, 2019). For instance, biochars that are produced at higher pyrolysis temperatures (>500°C) present higher surface areas because they tend to form more ordered structures, with a greater fraction of micropores (<1 µm) (Downie *et al.*, 2009; Keiluweit *et al.*, 2010; Peng *et al.*, 2011; Song and Guo, 2012). A dominant micropore fraction, which is aggregation dependent, is useful and important for increasing plant available water in soils (Brewer *et al.*, 2014). Moreover, applying biochar improves the binding interface of the soil, hence aggregation (Ajayi *et al.*, 2016)

The aggregation process and its outcomes influence the capacity and intensity parameters of the soil, and thus its functions. Since aggregation is a time and weather-based process, it is important to further evaluate how biochar amendment influences these parameters in relation to the soil type (varied texture). In specific terms, it is of interest to understand the dynamics of saturated hydraulic conductivity and water retention or pore-size distribution in biochar-amended soil, when it is subjected to repeated wetting and drying (Ajayi *et al.*, 2016; Diel *et al.*, 2019; Villagra-Mendoza and Horn, 2018a). Studies by Ajayi and Horn (2016) and Villagra-Mendoza and Horn (2018a) suggest that an improvement in soil structure occurs upon biochar addition, with direct consequences for hydraulic intensity parameters like saturated hydraulic conductivity. However, there is an increasing need to fully understand how biochar-moderated soil aggregation is influenced by some specific conditions that are related to biochar preparation, *e.g.*, the pyrolysis temperatures, feedstock size. Moreover, it is important to elucidate the progressive (ageing) effect of biochar-moderated aggregation on soil hydraulics, *e.g.*, the saturated and unsaturated hydraulic conductivity and water content in different soils based on the texture, *e.g.*, coarse vs. fine textured soil.

Another important property that affects intensity parameters, *e.g.*, water flux in biochar amended soil is the hydrophobicity (water repellency) behaviour. The repellency property of the soil affects water flux processes such as infiltration, evaporation, erosion and concomitantly, the soil hydrologic balance (Feng *et al.*, 2001; Wallis *et al.*, 1991). Water repellency usually occurs due to low energy at the soil-water interface. This is the result of the weak attraction between the molecules of the solid and liquid interface (Heslot *et al.*, 1990; Roy and McGill, 2002). Kholodov *et al.* (2015) reported that water repellency in the soil may be linked to soil structure. Since biochar amendments influence aggregation processes in the soil, it would be very interesting to also evaluate how biochar from different feedstock sizes at a particular temperature influence water repellency with varied textural properties. This is important as most studies (Ajayi *et al.*, 2016; Gray *et al.*, 2014; Kameyama *et al.*, 2019) have attributed water repellency in biochar amended soils to the hydrophobic nature of biochar, without considering how aggregation could influence

water repellency in these amended soils. A clearer understanding of the dynamic influence of biochar feedstocks and pyrolysis temperature, (if any), on the water attracting or repelling nature of the biochar produced is essential to furthering the understanding of the expected changes in biochar amended soil.

Several techniques have been developed to determine soil-water repellency including the water drop penetration time (WDPT), the capillary rise method (CRM), the molarity of an ethanol droplet (MED), and the sessile drop method (SDM). One of the more sensitive methods is the determination of water repellency through the contact angle. This angle is synonymously called the interface angle or wetting angle. High and low contact angles indicate a low and high solid surface energy or chemical affinity, which often result in a low and high degree of wetting, respectively.

Thus, the contact angle value describes and characterizes the possible wetting of the surface. When the contact angle is less than 90°, it shows that the surface is wetted and the surface is termed *hydrophilic*. Higher values imply that the surface is either not wettable or to a very moderate extent, and is thus termed *hydrophobic*. A contact angle of zero degrees will occur when the droplet has turned into a flat layer; which is termed completely hydrophilic.

The SDM provided a wider measurement range of the contact angle over other methods (Leelamanie *et al.*, 2008). Thus, the objectives of this study are to; (i) evaluate the aggregation effect in biochar amended soil by determining the dynamic changes in saturated hydraulic conductivity in 2 types of soils amended with biochar produced using two different feedstocks, (ii) determine the influence of these biochar types on soil water repellency in two soil types using the SDM, and (iii) determine the relationship between water repellency, aggregation and water content in soils amended with biochar produced using feedstocks of different sizes.

MATERIALS AND METHODS

Soil substrates, classified as silty loam and sandy loam were collected at 0-20 and 30-60 cm depths, at the Christian Albrechts University Farm Lindhof Germany. The silty loam consists of 4.2, 78.6 and 17.2% of sand, silt and clay, while the sandy loam soil consists of 59.4, 23.1 and 17.5% of sand, silt and clay, respectively. The soil texture was determined using a hydrometer method, as reported by (Zimmermann and Horn, 2020). The biochars used were derived from parts of the mango tree pyrolysed at a temperature of 550°C for 5 h and 1 h of residence time. Mango twig was used to produce biochar 1 (B₁), while the mango branch was used for the production of biochar 2 (B₂). Mango twig is the less substantial part of a mango tree, being the woody growth on which mango fruit develops, while the mango branches grow out of the trunk. The biochar produced from both feedstocks (distinguished by

size) were milled and sieved through a sieve of 630 μm . The specific surface area and microporosity of the biochar were determined using the Brunauer-Emmett-Teller (BET) procedure using an Quantachrome Autosorb-1 analyser. Detailed information about this procedure is reported in (Ajayi and Horn, 2016). Other chemical properties such as the nitrogen and organic carbon (OC) contents were determined using an elemental analyser, while the hydrophysical properties: bulk density and water holding capacity at 0 kPa were determined using standard procedures (ASTM E873-82, 2006; Faloye *et al.*, 2020). The basic properties of the biochars used for the study are presented in Table 1.

In order to characterize soil water content, the soil-biochar samples, which were prepared at different application rates of 0, 30, 45 and 60 g kg^{-1} , were moistened with distilled water. The 0, 30, 45 and 60 g kg^{-1} correspond to 0, 3, 4.5 and 6% application rates. The soil biochar samples were moistened at 0.05 g g^{-1} to ensure thorough mixing and were then repacked into 100 cm^3 metal cylinders (4 cm in height and 5.65 cm in diameter) at a uniform bulk density of 1.4 g cm^{-3} . Five replicates were prepared for each treatment. A description of the experimental treatments is shown in Table 2.

The soil samples were wetted by capillarity and dried at -60hPa and the soil water contents were determined at both matric potentials. After drying the samples at -60 hPa , they were rewetted at 0 hPa. This procedure was performed three times to ensure the structure formation of the soil-biochar mixture. After that, the measurement of saturated hydraulic

Table 1. Basic physicochemical and hydrological properties of the two biochar types used in this study. Means are given with standard deviations

Biochar type	N (%)	OC (%)	SSA ($\text{m}^2 \text{g}^{-1}$)	Bulk density (g cm^{-3})	WHC at 0 kPa ($\text{cm}^3 \text{cm}^{-3}$)
Biochar 1 (B ₁)	0.89±0.114	67.4±0.47	1.12±0.01	0.27±0.02	0.93±0.08
Biochar 2 (B ₂)	0.66±0.013	78.4±0.66	158±0.14	0.34±0.02	0.55±0.02

SSA – specific surface area; OC – organic carbon; N – nitrogen; WHC – water holding capacity.

Table 2. Definition of the experimental treatments

Treatment	Definition
S ₀	Unamended silt loam soil
S ₃ B ₁	Silt loam soil at 3% biochar using mango twig
S _{4.5} B ₁	Silt loam soil at 4.5% biochar using mango twig
S ₆ B ₁	Silt loam soil at 6% biochar using mango twig
S ₃ B ₂	Silt loam soil at 3% biochar using mango branch
S _{4.5} B ₂	Silt loam soil at 4.5% biochar using mango branch
S ₆ B ₂	Silt loam soil at 6% biochar using mango branch
SD ₀	Unamended sandy loam soil
SD ₃ B ₁	Sandy loam soil at 3% biochar using mango twig
SD _{4.5} B ₁	Sandy loam soil at 4.5% biochar using mango twig
SD ₆ B ₁	Sandy loam soil at 6% biochar using mango twig
SD ₃ B ₂	Sandy loam soil at 3% biochar using mango branch
SD _{4.5} B ₂	Sandy loam soil at 4.5% biochar using mango branch
SD ₆ B ₂	Sandy loam soil at 6% biochar using mango branch

conductivity was initiated. Saturated hydraulic conductivity (K_s) was measured using a falling-head permeameter, as described in Hartge and Horn (2016). Water flow through each soil sample was measured three times. The geometric means represent the K_s for a cycle, and this was repeated for five cycles. At the end of each cycle (after the completion of the measurements), the soil samples were air-dried for three days and subsequently dried in an oven at 30°C for 16 h. The purpose of the pre-drying stage was to prevent the soil samples from developing cracks, which may occur if the sample is suddenly subjected to high temperatures while it's still very wet. This crack may adversely alter the measurement of K_s . The magnitude of change in saturated hydraulic conductivity was determined to be the difference between the first cycle and the fifth cycle measurement.

After the last cycle of saturated hydraulic conductivity and air flow measurement was complete, the substrates were carefully repacked (without breaking the aggregates) into smaller rings (4.38 mm diameter and 1.43 mm height) in 5 replicates. Thereafter, each of these samples were positioned on the stage of a digital microscopic camera.

The contact angle of each substrate (treatment) sample was derived from the analysis of the images of the drop profiles through curve-fitting (using the optical method) the entire drop profile, using the Young-Laplace equation (Park *et al.*, 2013) as implemented using the Easy Drop Software. For each measurement, the water droplet is carefully dropped from a syringe placed above the soil surface in a controlled manner and the optical device (OCA20, DataPhysics, Filderstadt, Germany) records the drop movement with a high definition camera (Fig 1b). The camera has a frame rate of 250 s^{-1} . The droplets have an approximate volume of 8 μl and the contact area is accordingly about 4 mm^2 . The camera image (video clip) is analysed with the Easy Drop Software (Krüss GmbH), which allows for an accurate determination of the shape of the water droplet at

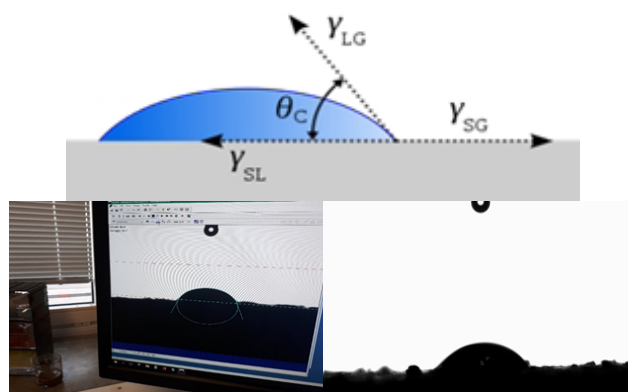


Fig. 1. An illustration of the sessile drop technique with a liquid droplet (a) partially wetting a solid substrate, (b) partially wetting a solid substrate during the experiment. θ_C – equilibrium contact angle, γ_{SG} – interfacial tension between the solid and gas, γ_{SL} – interfacial tension between the solid and liquid, γ_{LG} – interfacial tension between the liquid and gas.

first contact with the soil surface and its penetration into the soil. For each sample, measurements are made at 3 to 5 points depending on the size and flatness of the surface.

The means of the hydrophysical and contact angle data were separated using a Tukey test at a 5% level of significance. Minitab software was used to perform the post-hoc test. Also, a regression analysis between the contact angle and the soil water content was carried out using excel, version 2013.

RESULTS

The saturated hydraulic conductivity values decrease as the wetting-drying cycles increase (Table 3). The highest values of saturated hydraulic conductivity were recorded in the unamended soils, while the values significantly decreased as the amount of biochar added increased. The relative change in magnitude between the K_s measurements for cycle 1 and 5 was highest in the silty loam amended with B_2 while the highest decrease in saturated hydraulic conductivity was for the most part observed in sandy loam soil, amended with B_2 (Table 3).

Table 3 also shows the main and interactive effects between the biochar application rate and the biochar type on the saturated hydraulic conductivity. The main effect of the biochar application rate is significant with regard to the

Table 3. Saturated hydraulic conductivity (cm d^{-1}) of unamended and biochar amended soils

Treatment	Cycle 1	Cycle 2	Cycle 3	Cycle 4	Cycle 5	Magnitude of change (%)
S_0	44.24a	33.23a	39.93a	35.61a	46.20a	4.43
S_3B_1	28.06b	25.17bc	39.42a	26.74ab	25.07b	-10.7
$S_{4.5}B_1$	20.71b	20.03c	26.85b	24.37b	21.26b	2.66
S_6B_1	20.75b	27.99ab	22.83b	27.21ab	21.64b	3.84
S_0	44.24a	33.23a	39.93a	35.61a	56.20a	27.0
S_3B_2	26.69b	34.30a	37.97a	23.23bc	33.87a	26.9
$S_{4.5}B_2$	26.27b	41.84a	26.74a	27.18ab	33.63a	28.0
S_6B_2	29.97ab	31.39a	23.78a	16.90c	37.58a	25.4
SD_0	92.17a	113.16a	79.44a	60.42a	47.66a	-48.3
SD_3B_1	85.68a	59.23b	47.28ab	37.89a	31.70a	-63.0
$SD_{4.5}B_1$	55.41b	82.08ab	54.06ab	38.41a	34.79a	-37.2
SD_6B_1	30.37b	47.93b	31.36b	31.15a	28.07a	-7.5
SD_0	92.17a	113.16a	79.44a	60.42a	47.66a	-48.3
SD_3B_2	90.92a	67.79b	45.52ab	45.40a	43.87a	-51.7
$SD_{4.5}B_2$	59.43b	45.51bc	49.07ab	51.17a	43.63a	-26.6
SD_6B_2	59.27b	39.91c	38.52b	46.32a	37.58a	-36.6
Silt loam;	Sandy loam					
BR; $p = 0.0001$	BR; $p = 0.031$					
BT; $p = 0.052$	BT; $p = 0.125$					
BT *BR = 0.465	BT * BR = 0.445					

BR – Biochar Rate; BT – Biochar Type, means sharing a similar letter are statistically similar at a 5% level of significance using Tukey's test.

saturated hydraulic conductivity in both soil textural types, while the biochar type effect is insignificant. The interaction between the biochar application rate and biochar type is insignificant concerning the saturated hydraulic conductivity values in both soil textural types.

The water content increased with the amount of biochar added (Table 4). The water content at matric potentials of 0 and -60 hPa were significantly impacted by the biochar applications, as compared to the control. The water contents recorded at matric potentials of 0 and -60 hPa represent the results obtained during three repeated wetting and drying cycles. The difference in water content between the two biochar types at dosages of 0, 3, 4.5 and 6% was higher for B_1 , even as wetting and drying progresses (Table 4).

The water content and contact angle of the soil-biochar mixture are presented in Table 5. The water content increases with increases in the biochar application rates and decreases as the matric potential decreases. The measured contact angles were significantly higher in the amended soils as compared to the unamended soils for both types of biochar. It was also observed that in some cases, higher contact angles were observed in soils amended with mango twig biochar, as compared to the mango branch biochar. Moreover, the contact angle increases with the decrease in soil water content in the unamended and biochar amended soils. In most cases, the contact angle of the unamended soil and soil-biochar mixtures are $< 90^\circ$, which implies that they are hydrophilic in nature. The relationship between the soil water contents and the corresponding contact angle for both soil textural types amended with biochar at a matric potential of -6 kPa and below the wilting point are presented in Figures 2 and 3. Also, in most cases, the measured contact angle after wetting/drying was greater in the soil water condition that is below the wilting point. This observation was more obvious in the sandy loam soil (Table 4).

The relationship between the contact angle and the soil water content showed that the soil water content significantly ($p < 0.05$) influenced the contact angle for both soil types (textural difference) and with both types of biochar (feedstock size difference). Also, the coefficient of determination ($R^2 > 0.5$) was fairly high in both cases. A graphical

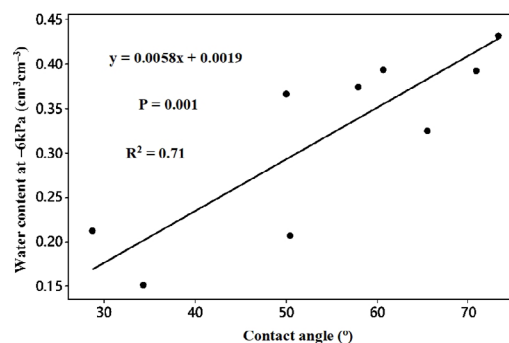


Fig. 2. Relationship between the contact angle and water content at -6 kPa in the pooled data of silt loam and sandy loam soil amended with both biochar types

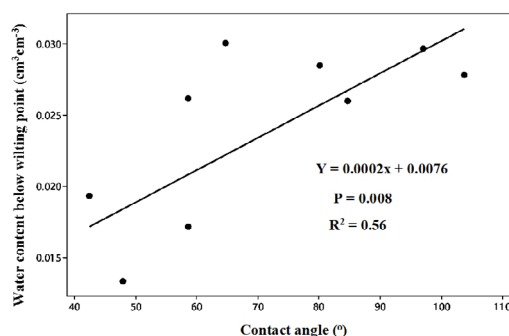


Fig. 3. Relationship between the contact angle and water content below the wilting point in the pooled data of silt loam and sandy loam soil amended with both biochar types.

presentation of the relationship also indicated a positive slope, which implies that as the soil water content increases, the contact angle also increases.

DISCUSSION

This study focused on the evaluation of changes in aggregation by determining the water repellency index (contact angle), dynamic saturated hydraulic conductivity and water content at saturation due to absorption.

Biochar gluing attributes make soils rigid due to the binding compound present in them (Githinji, 2014). Increases in the amount of biochar added resulted in a saturated hydraulic conductivity decrease due to the infilling of the pores,

Table 4. Effects of biochar on the soil water content ($\text{cm}^3 100 \text{ cm}^{-3}$) as influenced by wetting and drying (Values in parenthesis represent the difference between the water content of biochar 1 and biochar 2 at the same application rates)

Treatment	Cycle 1		Cycle 2		Cycle 3	
	Matric potential (hPa)					
	0	-60	0	-60	0	-60
S	54.29b	47.87b	53.64c	47.46d	54.31d	47.86d
S ₃ B ₁	57.99ab(1.97)	51.56ab(1.04)	58.08b(1.28)	52.38c(1.48)	58.31c(0.1)	52.62c(1.68)
S _{4.5} B ₁	60.49a(-1.25)	54.12a(0.5)	59.68a(1.08)	54.24b(1.37)	59.74b(0.24)	54.82b(2.04)
S ₆ B ₁	61.61a(-1.34)	55.97a(1.0)	60.81a(0.97)	56.21a(1.72)	61.45a(0.69)	56.80a(2.44)
S	54.29c	47.87d	53.64c	47.46d	54.31c	47.86d
S ₃ B ₂	59.96b	50.52c	56.80b	50.90c	58.21b	50.94c
S _{4.5} B ₂	61.74a	53.62b	58.60a	52.87b	59.50ab	52.78b
S ₆ B ₂	62.95a	54.97a	59.84a	54.49a	60.76a	54.36a
SD	47.35a	20.55c	36.51b	21.30c	35.79c	20.97c
SD ₃ B ₁	49.62a(3.06)	28.84b(3.58)	42.84a(2.84)	30.08b(5.22)	41.88b(3.44)	29.54b(4.77)
SD _{4.5} B ₁	49.20a(0.70)	32.59a(4.74)	44.42a(1.13)	36.30a(10.06)	44.02ab(2.69)	35.40a(9.09)
SD ₆ B ₁	48.80a(-0.34)	35.74a(4.14)	45.49a(1.51)	37.74a(7.98)	45.61a(3.18)	37.99a(8.47)
SD	47.35ab	20.55d	36.51c	21.30d	35.79c	20.97d
SD ₃ B ₂	46.56b	25.26c	40.03b	24.86c	38.44b	24.77c
SD _{4.5} B ₂	48.50ab	27.85b	43.29a	26.24b	41.33a	26.31b
SD ₆ B ₂	49.14a	31.60a	43.98a	29.76a	42.43a	29.52a

Explanations as in Table 3.

Table 5. Contact angles (°) of soil-biochar mixtures at different matric potentials and water contents ($\text{cm}^3 \text{ cm}^{-3}$)

Treatment	Contact angle at -6 kPa	Water content at -6 kPa	Contact angle at wilting point	Water content at wilting point -15000 hPa	Contact angle at wilting point after wetting-drying	Water content at wilting point -15000 hPa after wetting-drying
S ₀	50b	0.366	84.6b	0.026	52.65c	0.0244
S ₃ B ₁	60.7ab	0.394	103.7a	0.0279	68.83b	0.0261
S _{4.5} B ₁	73.3a	0.432	80.1b	0.0285	89.8a	0.0268
S ₆ B ₁	ND	ND	ND	ND	ND	ND
S ₀	50b	0.366	84.6b	0.026	52.65c	0.0244
S ₃ B ₂	70.9a	0.392	97.1a	0.0297	74.11b	0.0259
S _{4.5} B ₂	57.9ab	0.374	64.6b	0.0301	70.75b	0.0285
S ₆ B ₂	ND	ND	ND	ND	ND	ND
SD ₀	34.3c	0.152	47.9ab	0.0134	81.92b	0.0122
SD ₃ B ₁	65.5a	0.325	58.5a	0.0262	55.43a	0.0241
SD _{4.5} B ₁	ND	ND	ND	ND	ND	ND
SD ₆ B ₁	ND	ND	ND	ND	ND	ND
SD ₀	34.3c	0.152	47.9ab	0.0134	81.92b	0.0122
SD ₃ B ₂	28.8c	0.213	42.4b	0.0194	75.08b	0.0178
SD _{4.5} B ₂	50.5b	0.207	58.5a	0.0172	75.78b	0.0157
SD ₆ B ₂	ND	ND	ND	ND	ND	ND

ND – means not determined. Other explanations as in Table 3.

with K_s also decreasing with increases in wetting/drying in the sandy loam soil. But the opposite was the case in the silt loam soil, the observed increase in saturated hydraulic conductivity as wetting/drying progresses may be attributed to the rearrangement of the soil-biochar particles (Sun *et al.*, 2013). The improvement in soil structure upon biochar addition, particularly in the silt loam soil was evident after the wetting/drying cycles, which may be attributed to the rearrangement of the soil particles. However, the behaviour of the soil upon biochar incorporation depends on texture as shown in our study. In sandy loam soil-biochar mixtures, saturated hydraulic conductivity decreased with increasing amounts of added biochar, while there was a general increase in the case of silt loam soil. These results are in agreement with the reports of (Bodner *et al.*, 2013). The addition of biochar enables the sandy loam soil to resist/withstand capillary stress because the saturated hydraulic conductivity after repeated wetting and drying remained constant in the biochar-amended sandy loam soil. The magnitude of change decreases as the dosage of biochar added increases, thus explaining the improved rigidity of sandy loam soil when biochar was added. This rigidity could be increased in the sandy loam soil treated with B_1 . One possible explanation for the lower magnitude of change in K_s may be attributed to menisci forces (forces of adhesion and cohesion). The addition of biochar to the sandy loam soil may have increased the adhesive force; the force of attraction between different substances/molecules. The adhesive force between a molecule of the sandy soil and biochar may be greater than the cohesive force of the water; this is due to the forces of cohesion between the water molecules. It might also be greater than the capillary force. Therefore, a higher application rate of biochar improved the strength of the sandy loam soil, thereby enabling the biochar amended sandy soil to be relatively more cohesive in terms of rigidity. However, there were differing impacts according to the biochar type added in these processes. The differences in the behaviour of the two biochar types are based on their binding attributes, which is also dependent on the chemical compounds that they are composed of (Das and Sarmah, 2015; Dunnigan *et al.*, 2018; Dunning *et al.*, 2018; Kinney *et al.*, 2012). The improved binding observed for B_1 may be attributed to some sticky organic compounds present in B_1 but absent from B_2 or present in smaller amounts (Das and Sarmah, 2015; Dunnigan *et al.*, 2018; Kinney *et al.*, 2012).

The observed lower magnitude of the change in K_s as recorded in the silty loam soil amended with mango twig biochar as compared to that of B_2 may also be attributed to a higher binding effect (Demirbas, 2004). Also, the increased K_s value in the silty loam soil as wetting/drying progresses is expected because the increased pore water pressure and the alteration in the menisci forces may have resulted in the rearrangement and orientation of the internal particles, thus resulting in the formation of aggregates and possible inter-aggregate cracks. The re-orientation of the

internal particles may be possible due to water flow through the silty loam soil-biochar mixture. This is a result of the smaller than average particle size of the silty loam, which is dominated by silt of size 2–63 μm compared to sandy loam which is dominated by sand of size 63–2000 μm . Similar observations were recorded by Ajayi *et al.* (2016). These processes combined together may explain the increased saturated hydraulic conductivity observed in silt loam – biochar amended soil as wetting and drying progresses. Improving water flow, particularly with the use of biochar in the silt loam soil is important for solving the problem of soil aeration and drainage problems in finer texture soils. This is confirmed by the wetting and drying cycles which simulate the seasonal changes scenario, even under extreme conditions (saturation and oven-drying at 30°C). Also, it is important to note that, for rearrangements of particles to occur, soil-biochar mixtures must be subjected to wetting/drying cycles (Bodner *et al.*, 2013; Peng *et al.*, 2007). The results of our study corroborate the findings of Mubarak *et al.* (2009), who state that biochar addition improves water flow, due to the alteration in pore structure created over the course of the wetting/drying process (Peng *et al.*, 2007). Also, increased porosity with wetting/drying cycles was reported by Peng *et al.* (2007) due to increases in the macropore fraction. The increased macropore fraction may possibly explain the enhanced saturated hydraulic conductivity in the silt loam soil, as wetting/drying progresses. The drying process caused the soil porosity to decrease (Leij *et al.*, 2002), leading to the formation of aggregates and intensifying the quantity of finer pores. The formation of aggregates increased more in the biochar amended soil as the amount of biochar increased (Bodner *et al.*, 2013).

In the sandy loam soil – coarse textured soil, the particle arrangement irreversibly collapsed, irrespective of the amount of biochar added. This occurs as a result of the pulling effect of the menisci forces which was induced as the wetting/drying cycle intensifies. By contrast, the menisci forces caused the rearrangement and continuous reformation of the soil structure as the wetting/drying cycles progress in the silt loam soil. This is because of the presence of smaller particles as compared to the relatively coarser sandy loam, therefore their movement resulting from hydraulic forces could be intensified as a result of capillarity, both during wetting and drying phases. Due to hydraulic forces, their movement may also have induced particle re-organization, re-orientation and re-arrangement. Moreover, biochar addition further modifies the shape and orientation of the amended soils and their arrangement in the increasing order of application (Ajayi *et al.*, 2016).

The increase of soil water repellency results in a substantial reduction in infiltration rates and increased runoff. Water repellency is a common phenomenon in soils, thereby affecting water flow into the soil. Fine textured soils show some degree of repellency due to the formation of aggregates (Doerr *et al.*, 2000). The hydrophilic conditions

of the two textural soil types was evident from the contact angle of $<90^\circ$ in both the amended and unamended soils. The hydrophilic soil conditions of the unamended sandy loam soil facilitated the easy flow of water into the soil although hydrophilicity decreases with increases in biochar application, thereby reducing the infiltration of water into the soil. This was confirmed through the measured contact angle, which presents significantly higher values when compared to the unamended soils. As the sandy loam soil undergoes continuous wetting and drying, it becomes less hydrophilic due to the binding effects of the added biochar. This effect was particularly more pronounced in the soil amended with biochar produced using mango twig. This result may not only be attributed to the degree of hydrophobicity of the biochar used, but it should also be noted that the interactions within the biochar impacted and altered the accessibility of the particle surfaces and the total amount in combination with the swell-shrink effects. The greater the binding effects between the soil-biochar mixture, due to the differences in biochar type, the more the degree of adhesion increases (between water molecules and soil-biochar mixtures), thereby resulting in increased water retention (Alghamdi *et al.*, 2020).

An additional factor which may affect the aggregation effect in soils amended with biochar is the specific surface area of the biochar (Keiluweit *et al.*, 2010; Kameyama *et al.*, 2019), but its particular impact on aggregation improvement, when feedstocks of different types and sizes are used, has scarcely been reported to date. The improved aggregation effect using mango twig with a lower specific surface area may be attributed to some binding compound contained in B₁, which resulted in better aggregation. This is evidenced in the wetting/drying cycle, with a higher water content being observed, and the differences in water content in soil amended with B₂ becoming clearer and more obvious as the wetting and drying cycles progress. Due to the greater aggregation effect, the soil was more repellent to water.

Similar to the result of our study, Villagra-Mendoza and Horn (2018a) reported a decrease in the infiltration rate as wetting/drying progresses. This showed that the soil becomes more water repellent as the wetting/drying process is repeated due to aggregation. This is evident from the increase in soil water content obtained at the 0 and -6 kPa matric potential, as the wetting/drying cycle progresses. Therefore, the differences in soil water content as wetting/drying progresses may explain the aggregation effect, with higher increases in water content recorded in soil amended with mango twig as compared to those soils amended with mango branch. The results from our study show that the biochar effect on water repellency in soils is textural type dependent (Githinji, 2014), particularly when subjected to intense wetting/drying. Also, the water repellency determination due to aggregation is important for soil water content prediction and evaluation in biochar amended soils. This is evident from the favourable relationship ($R^2 > 0.5$) and

significant effect that was established between the contact angle (water repellency index) and soil water content in our study. Also, the positive relationship between the contact angle and soil water content, even as the biochar dosage increases at different matric potentials, showed that aggregation is important for improving water retention capacity in soils amended with Biochar.

In addition, the contact angle values depend on the soil matric potential. The higher values of the contact angle reported at more negative matric potentials (at the wilting point) as compared to those measured at -6 kPa explained this phenomenon/occurrence. The higher contact angle under drier conditions may be attributed to the redistribution of organic molecules that restored hydrophobicity in both soil textural types (sandy loam and silt loam) to some degree (Doerr *et al.*, 2000). The restored water repellency was more evident in soils amended with biochar produced using mango twig, this was probably due to the binding effect of biochar resulting in aggregation. Overall, the greater tendency to aggregate, binding effect and water repellency observed in soil amended with B₁ as opposed to B₂, may be the result of the sticky/gluing compound present in B₁.

CONCLUSIONS

1. Saturated hydraulic conductivity decreases in both sandy loam and silt loam soils amended with biochar produced using mango twig and branch as feedstocks. The decrease in saturated hydraulic conductivity in the biochar amended soils was attributed to a collapse of the pore system and an increase in the bulk density due to shrinkage without further crack formation. The magnitude of the decrease in saturated hydraulic conductivity was more pronounced in the sandy loam soil amended with biochar produced using twig, as compared to the biochar produced using mango branch, as wetting and drying progresses. If crack formation occurs, the saturated hydraulic conductivity increases.
2. The binding effects of the two biochar types may be responsible for the improved soil rigidity, thus enabling the soil to overcome/reduce capillary/hydraulic stress due to repetitive/continuous wetting and drying.
3. The aggregation effect may be explained by the enhanced improvement in soil water content upon biochar addition at different matric potentials, which keeps the Chi factor higher and causes more pronounced hydraulic stresses during wetting/drying
4. The binding and aggregation effects explain the higher contact angle (index of hydrophobicity/water repellency or aggregation) observed in biochar produced using mango twig and branch, respectively.
5. Hydrophobicity/water repellency increases as aggregation increases in biochar amended soils, thus resulting in an increased water retention capacity.

Conflict of interest: The authors declare no conflict of interest.

REFERENCES

- Ajayi A.E., Holthusen D., and Horn R., 2016.** Changes in microstructural behaviour and hydraulic functions of biochar amended soils. *Soil Till. Res.*, 155, 66-175, <https://doi.org/10.1016/j.still.2015.08.007>
- Ajayi A.E. and Horn R., 2016.** Modification of chemical and hydrophysical properties of two texturally differentiated soils due to varying magnitudes of added biochar. *Soil Till. Res.*, 164, 34-44, <https://doi.org/10.1016/j.still.2016.01.011>
- Alghamdi A.G., Alkhasha A., and Ibrahim H.M., 2020.** Effect of biochar particle size on water retention and availability in a sandy loam soil. *J. Saudi Chem. Soc.*, 24(12), 1042-1050, <https://doi.org/10.1016/j.jscs.2020.11.003>
- ASTM E873-82, 2006.** Standard test method for bulk density of densified particulate biomass fuels. *Annual Book of ASTM Standards*, 82 (Reapproved).
- Baiamonte G., Crescimanno G., Parrino F., and De Pasquale C., 2019.** Effect of biochar on the physical and structural properties of a desert sandy soil. *Catena*, 175, 294-303, <https://doi.org/10.1016/j.catena.2018.12.019>
- Bodner G., Scholl P., and Kaul H.P., 2013.** Field quantification of wetting-drying cycles to predict temporal changes of soil pore size distribution. *Soil Till. Res.*, 133, 1-9, <https://doi.org/10.1016/j.still.2013.05.006>
- Brewer C.E., Chuang V.J., Masiello C.A., Gonnermann H., Gao X., Dugan B., Driver L.E., Panzacchi P., Zygourakis K., and Davies C.A., 2014.** New approaches to measuring biochar density and porosity. *Biomass and Bioenerg.*, 66, 76-185, <https://doi.org/10.1016/j.biombioe.2014.03.059>
- Das O. and Sarmah A.K., 2015.** The love-hate relationship of pyrolysis biochar and water: A perspective. *Sci. Tot. Environ.*, 512-513, 682-685, <https://doi.org/10.1016/j.scitotenv.2015.01.061>
- de Jesus Duarte S., Glaser B., and Cerri C.E.P., 2019.** Effect of biochar particle size on physical, hydrological and chemical properties of loamy and sandy tropical soils. *Agronomy*, 9(4), 165, <https://doi.org/10.3390/agronomy9040165>
- Demirbas A., 2004.** Effects of temperature and particle size on biochar yield from pyrolysis of agricultural residues. *J. Anal. Appl. Pyrolysis*, 72(2), 243-248, <https://doi.org/10.1016/j.jaap.2004.07.003>
- Diel J., Vogel H.J., and Schlüter S., 2019.** Impact of wetting and drying cycles on soil structure dynamics. *Geoderma*, 345, 63-71, <https://doi.org/10.1016/j.geoderma.2019.03.018>
- Doerr S.H., Shakesby R.A., and Walsh R.P. D., 2000.** Soil water repellency: Its causes, characteristics and hydro-geomorphological significance. *Earth-Sci. Rev.*, 51(1-4), 33-65, [https://doi.org/10.1016/S0012-8252\(00\)00011-8](https://doi.org/10.1016/S0012-8252(00)00011-8)
- Downie A., Crosky A., and Munroe P., 2009.** Physical properties of biochar. In: *Biochar for environmental management* (Eds J. Lehmann and S. Joseph). Science and Technology, Earthscan, London, 13-32.
- Drellich J., 2013.** Guidelines to measurements of reproducible contact angles using a sessile-drop technique. *Surf. Innov.*, 1(4), 248-254, <https://doi.org/10.1680/si.13.00010>
- Dunnigan L., Ashman P.J., Zhang X., and Kwong C.W., 2018.** Production of biochar from rice husk: Particulate emissions from the combustion of raw pyrolysis volatiles. *J. Clean. Prod.*, 172, 1639-1645, <https://doi.org/10.1016/j.jclepro.2016.11.107>
- Dunning C.M., Black E., and Allan R.P., 2018.** Later wet seasons with more intense rainfall over Africa under future climate change. *J. Clim.*, 31(23), 9719-9738, <https://doi.org/10.1175/JCLI-D-18-0102.1>
- Esmaelnejad L., Shorafa M., Gorji M., and Hosseini S. mossa., 2017.** Impacts of Woody Biochar Particle Size on Porosity and Hydraulic Conductivity of Biochar-Soil Mixtures: An Incubation Study. *Commun. Soil Sci. Plant Anal.*, 48(14), 1710-1718, <https://doi.org/10.1080/00103624.2017.1383414>
- Faloye O.T., Ajayi A.E., Alatise M.O., Ewulo B.S., and Horn R., 2020.** Maize Growth and Yield Modelling Using AquaCrop Under Deficit Irrigation with Sole and Combined Application of Biochar and Inorganic Fertiliser. *J. Soil Sci. Plant Nutr.*, 20(4), 2440-2453, <https://doi.org/10.1007/s42729-020-00310-1>
- Feng G.L., Letey J., and Wu L., 2001.** Water Ponding Depths Affect Temporal Infiltration Rates in a Water-Repellent Sand. *Soil Sci. Soc. Am. J.*, 65(2), 315-320, <https://doi.org/10.2136/sssaj2001.652315x>
- Githinji L., 2014.** Effect of biochar application rate on soil physical and hydraulic properties of a sandy loam. *Arch. Agron. Soil Sci.*, 60(4), 457-470, <https://doi.org/10.1080/03650340.2013.821698>
- Gray M., Johnson M.G., Dragila M.I., and Kleber M., 2014.** Water uptake in biochars: The roles of porosity and hydrophobicity. *Biomass Bioenerg.*, 61, 196-205, <https://doi.org/10.1016/j.biombioe.2013.12.010>
- Guo J. and Lua A.C., 1998.** Characterization of chars pyrolyzed from oil palm stones for the preparation of activated carbons. *J. Anal. Appl. Pyrolysis*, 46(2), 113-125, [https://doi.org/10.1016/S0165-2370\(98\)00074-6](https://doi.org/10.1016/S0165-2370(98)00074-6)
- Hartge K.H. and Horn R., 2016.** *Essential Soil Physics*. Schweizerbart Science Publisher. Stuttgart, Germany.
- Heslot F., Cazabat A.M., Levinson P., and Frayse N., 1990.** Experiments on wetting on the scale of nanometers: Influence of the surface energy. *Phys. Rev. Lett.*, 65(5), 599, <https://doi.org/10.1103/PhysRevLett.65.599>
- Islam M.U., Jiang F., Guo Z., and Peng, X., 2021.** Does biochar application improve soil aggregation? A meta-analysis *Soil Till. Res.*, 209, 104926, <https://doi.org/10.1016/j.still.2020.104926>
- Kameyama K., Miyamoto T., and Iwata Y., 2019.** The preliminary study of water-retention related properties of biochar produced from various feedstock at different pyrolysis temperatures. *Materials*, 12(11), 1732, <https://doi.org/10.3390/ma12111732>
- Keiluweit M., Nico P.S., Johnson M., and Kleber M., 2010.** Dynamic molecular structure of plant biomass-derived black carbon (biochar). *Envir. Sci. Technol.*, 44(4), 1247-1253, <https://doi.org/10.1021/es9031419>
- Kholodov V.A., Yaroslavtseva N.V., Yashin M.A., Frid A.S., Lazarev V.I., Tyugai Z.N., and Milanovskiy E.Y., 2015.** Contact angles of wetting and water stability of soil structure. *Eurasian Soil Sci.*, 48(6), 600-607, <https://doi.org/10.1134/S106422931506006X>
- Kinney T.J., Masiello C.A., Dugan B., Hockaday W.C., Dean M.R., Zygourakis K., and Barnes R.T., 2012.** Hydrologic properties of biochars produced at different temperatures. *Biomass Bioenerg.*, 41, 34-43, <https://doi.org/10.1016/j.biombioe.2012.01.033>

- Leelamanie D.A. L., Karube J., and Yoshida A., 2008.** Characterizing water repellency indices: Contact angle and water drop penetration time of hydrophobized sand. *Soil Sci. Plant Nutr.*, 54(2), 179-187, <https://doi.org/10.1111/j.1747-0765.2007.00232.x>
- Leij F.J., Ghezzehei T.A., and Or D., 2002.** Modeling the dynamics of the soil pore-size distribution. *Soil Till. Res.*, 64(1-2), 61-78, [https://doi.org/10.1016/S0167-1987\(01\)00257-4](https://doi.org/10.1016/S0167-1987(01)00257-4)
- Lua A.C., Yang T., and Guo J., 2004.** Effects of pyrolysis conditions on the properties of activated carbons prepared from pistachio-nut shells. *J. Anal. Appl. Pyrolys.*, 72(2), 279-287, <https://doi.org/10.1016/j.jaap.2004.08.001>
- Mubarak A.R., Ragab O.E., Ali A.A., and Hamed N.E., 2009.** Short-term studies on use of organic amendments for amelioration of a sandy soil. *African J. Agric. Res.*, 4(7), 621-627.
- Park J., Park J., Lim H., and Kim H.Y., 2013.** Shape of a large drop on a rough hydrophobic surface. *Phys. Fluids*, 25(2), 022102, <https://doi.org/10.1063/1.4789494>
- Peng X., Horn R., and Smucker A., 2007.** Pore Shrinkage Dependency of Inorganic and Organic Soils on Wetting and Drying Cycles. *Soil Sci. Soc. Am. J.*, 71(4), 1095-1104, <https://doi.org/10.2136/sssaj2006.0156>
- Peng X., Ye L.L., Wang C.H., Zhou H., and Sun B., 2011.** Temperature- and duration-dependent rice straw-derived biochar: Characteristics and its effects on soil properties of an Ultisol in southern China. *Soil Till. Res.*, 112(2), 159-166, <https://doi.org/10.1016/j.still.2011.01.002>
- Roy J.L. and McGill W.B., 2002.** Assessing soil water repellency using the molarity of ethanol droplet (MED) test. *Soil Sci.*, 167(2), 83-97, <https://doi.org/10.1097/00010694-200202000-00001>
- Song W., and Guo M., 2012.** Quality variations of poultry litter biochar generated at different pyrolysis temperatures. *J. Anal. Appl. Pyrolys.*, 94, 138-145, <https://doi.org/10.1016/j.jaap.2011.11.018>
- Sun Z., Moldrup P., Elsgaard L., Arthur E., Bruun E.W., Hauggaard-Nielsen H., and De Jonge L.W., 2013.** Direct and indirect short-term effects of biochar on physical characteristics of an arable sandy loam. *Soil Sci.*, 178(9), 465-473, <https://doi.org/10.1097/SS.0000000000000010>
- Villagra-Mendoza K., and Horn R., 2018a.** Effect of biochar addition on hydraulic functions of two textural soils. *Geoderma*, 326, 88-95, <https://doi.org/10.1016/j.geoderma.2018.03.021>
- Villagra-Mendoza K., and Horn R., 2018b.** Effect of biochar on the unsaturated hydraulic conductivity of two amended soils. *Int. Agrophys.*, 32(3), 373-378, <https://doi.org/10.1515/intag-2017-0025>
- Wallis M.G., Scotter D.R., and Horne D.J., 1991.** An evaluation of the intrinsic sorptivity water repellency index on a range of New Zealand soils. *Austral. J. Soil Res.*, 29(3), 353-362, <https://doi.org/10.1071/SR9910353>
- Woolf D., Amonette J.E., Street-Perrott F.A., Lehmann J., and Joseph S., 2010.** Sustainable biochar to mitigate global climate change. *Nat. Commun.*, 1, 56, <https://doi.org/10.1038/ncomms1053>
- Zimmermann I. and Horn R., 2020.** Impact of sample pretreatment on the results of texture analysis in different soils. *Geoderma*, 371, 114379, <https://doi.org/10.1016/j.geoderma.2020.114379>